

Electronic Supplementary Material (ESI) for Nanoscale.  
This journal is © The Royal Society of Chemistry 2020

## Supporting information

### **Pore Structure Regulation of Biomass-Derived Carbon Materials for Enhanced Supercapacitor Performance**

He Xu<sup>a</sup>, Liyuan Wang<sup>b, \*</sup>, Yi Zhang<sup>a</sup>, Ye Chen<sup>b</sup>, Shuyan Gao<sup>a,b,\*</sup>

<sup>a</sup>.School of Chemistry and Chemical Engineering, Henan Normal University, Xinxiang 453007, PR China.

<sup>b</sup>.School of Materials Science and Engineering, Henan Normal University, Xinxiang, Henan, 453007, PR China. E-mail address: wangliyuan5450@163.com (L. Wang); shuyangao@htu.cn (S. Gao)

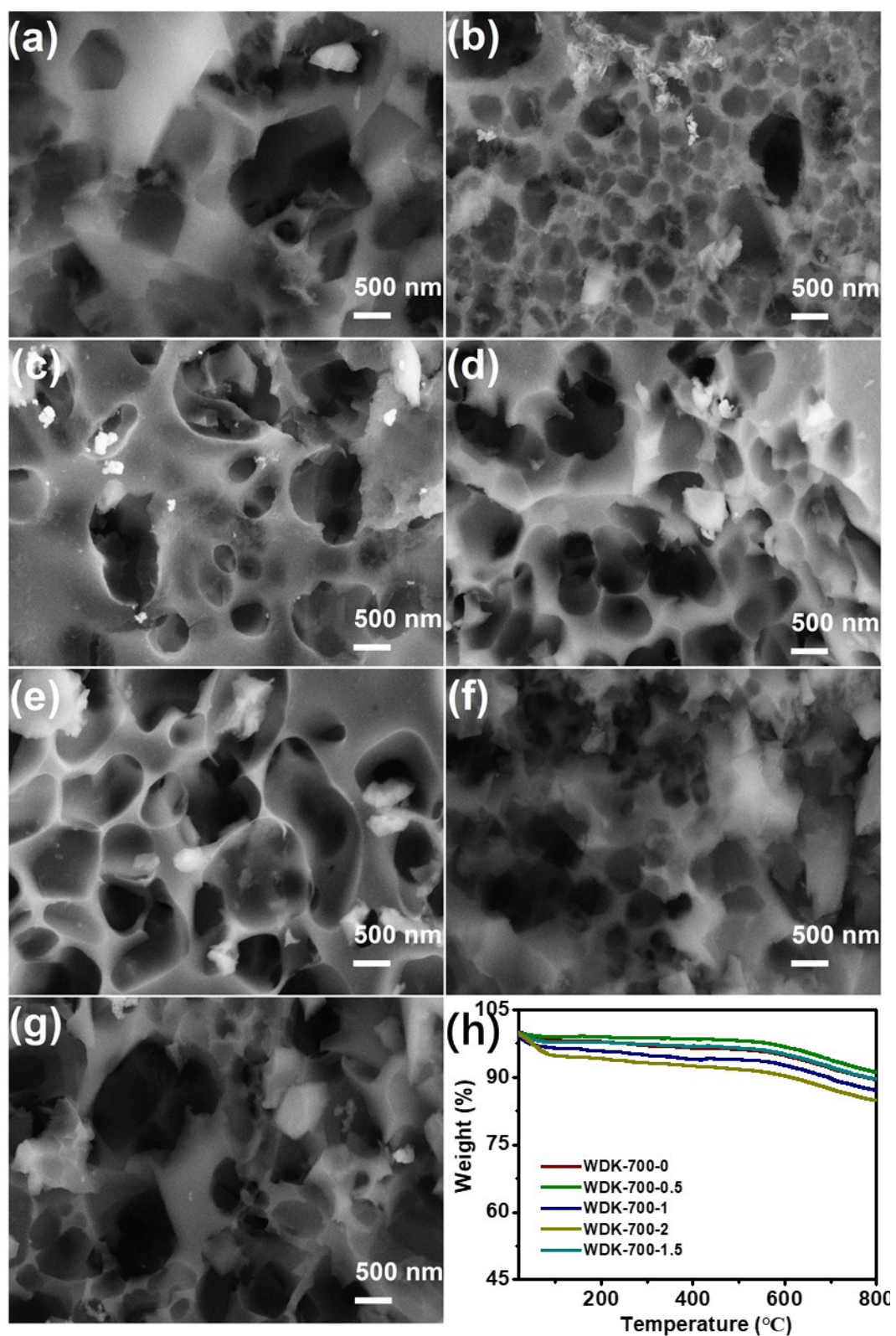


**Fig. S1** SEM images of WDK-700-1 (a), WDK-700-0 (b), WDK-700-0.5 (c), WDK-700-1.5 (d), WDK-700-2 (e), WDK-600-1 (f), WDK-800-1 (g), and TGA curve of samples in N<sub>2</sub> atmosphere (h).

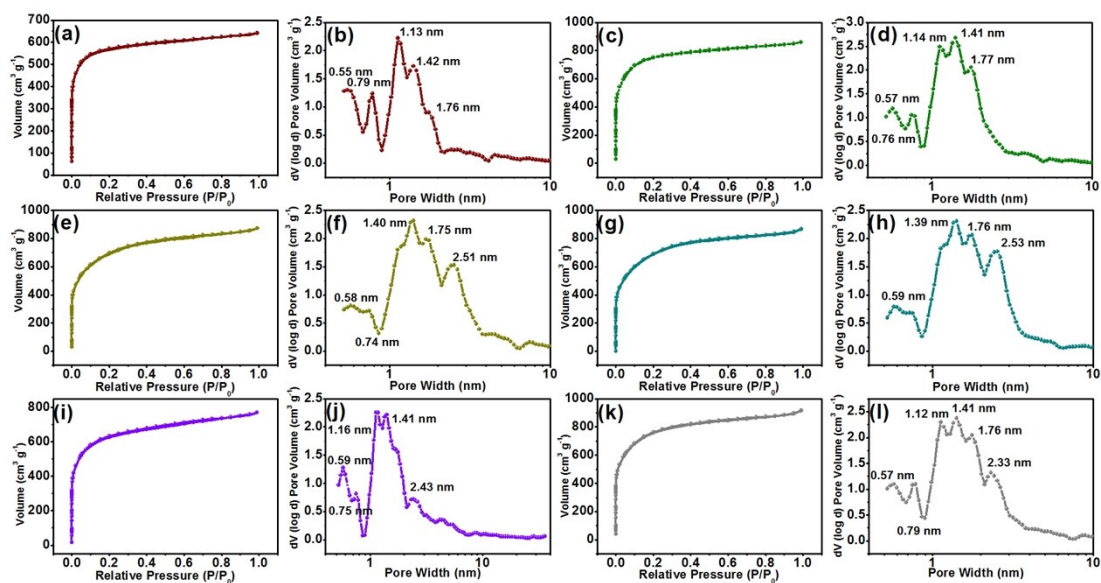


**Fig. S2** (a) N<sub>2</sub> adsorption/desorption curve of WDK-700-0, (b) pore size distribution of WDK-700-0, (c) N<sub>2</sub> adsorption/desorption curve of WDK-700-0.5, (d) pore size distribution of WDK-700-0.5, (e) N<sub>2</sub> adsorption/desorption curve of WDK-700-1.5, (f) pore size distribution of WDK-700-1.5, (g) N<sub>2</sub> adsorption/desorption curve of WDK-700-2, (h) pore size distribution of WDK-700-2, (i) N<sub>2</sub> adsorption/desorption curve of WDK-600-1, (j) pore size distribution of WDK-600-1, (k) N<sub>2</sub> adsorption/desorption curve of WDK-800-1, (l) pore size distribution of WDK-800-1.

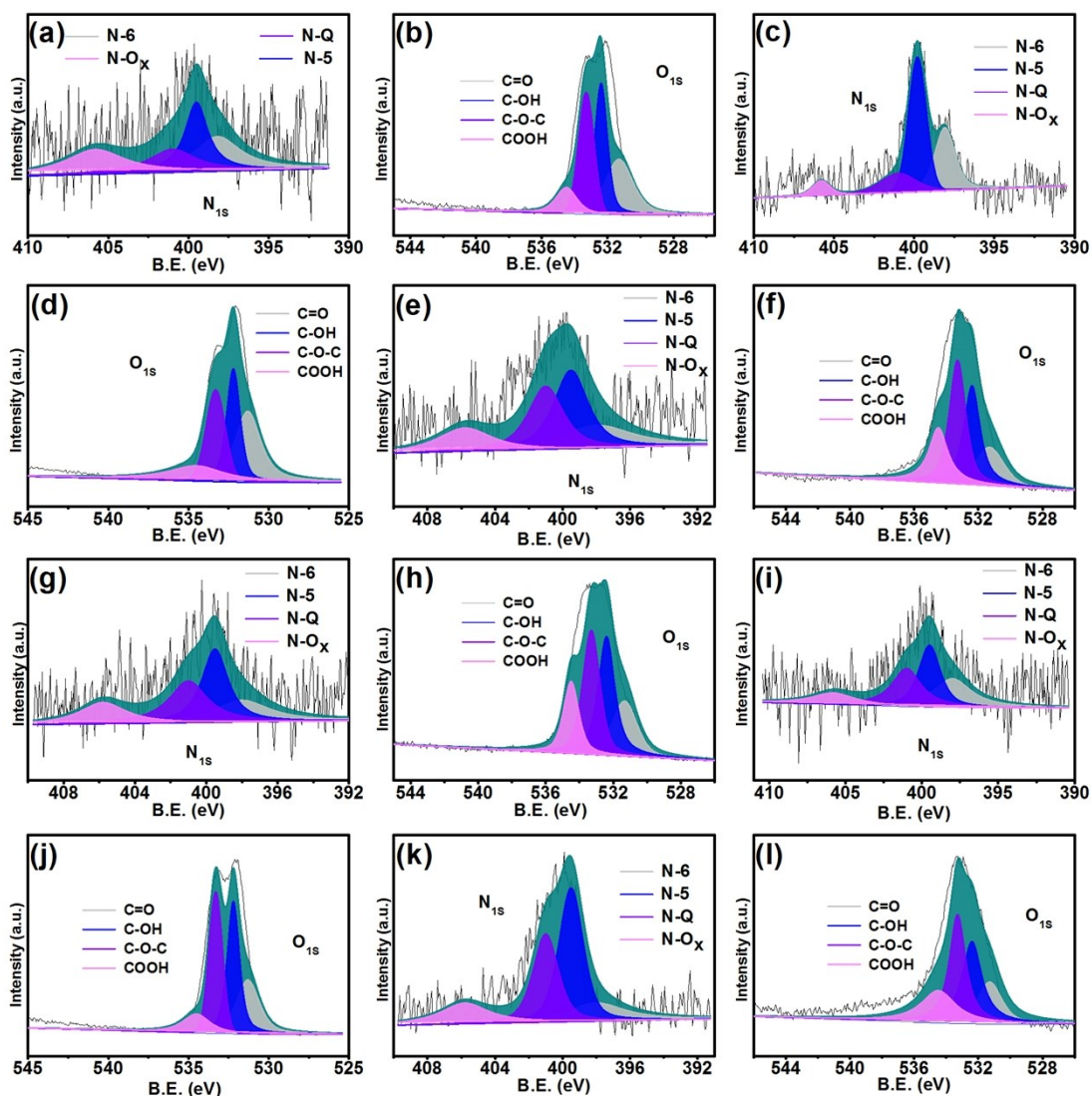


**Fig. S3** (a)  $N_{1s}$  and (b)  $O_{1s}$  high-resolution XPS spectra of WDK-700-0 with deconvoluted peaks, (c)  $N_{1s}$  and (d)  $O_{1s}$  high-resolution XPS spectra of WDK-700-0.5 with deconvoluted peaks, (e)  $N_{1s}$  and (f)  $O_{1s}$  high-resolution XPS spectra of WDK-700-1.5 with deconvoluted peaks, (g)  $N_{1s}$  and (h)  $O_{1s}$  high-resolution XPS spectra of WDK-700-2 with deconvoluted peaks, (i)  $N_{1s}$  and (j)  $O_{1s}$  high-resolution XPS spectra of WDK-600-1 with deconvoluted peaks, (k)  $N_{1s}$  and (l)  $O_{1s}$  high-resolution XPS spectra of WDK-800-1 with deconvoluted peaks.

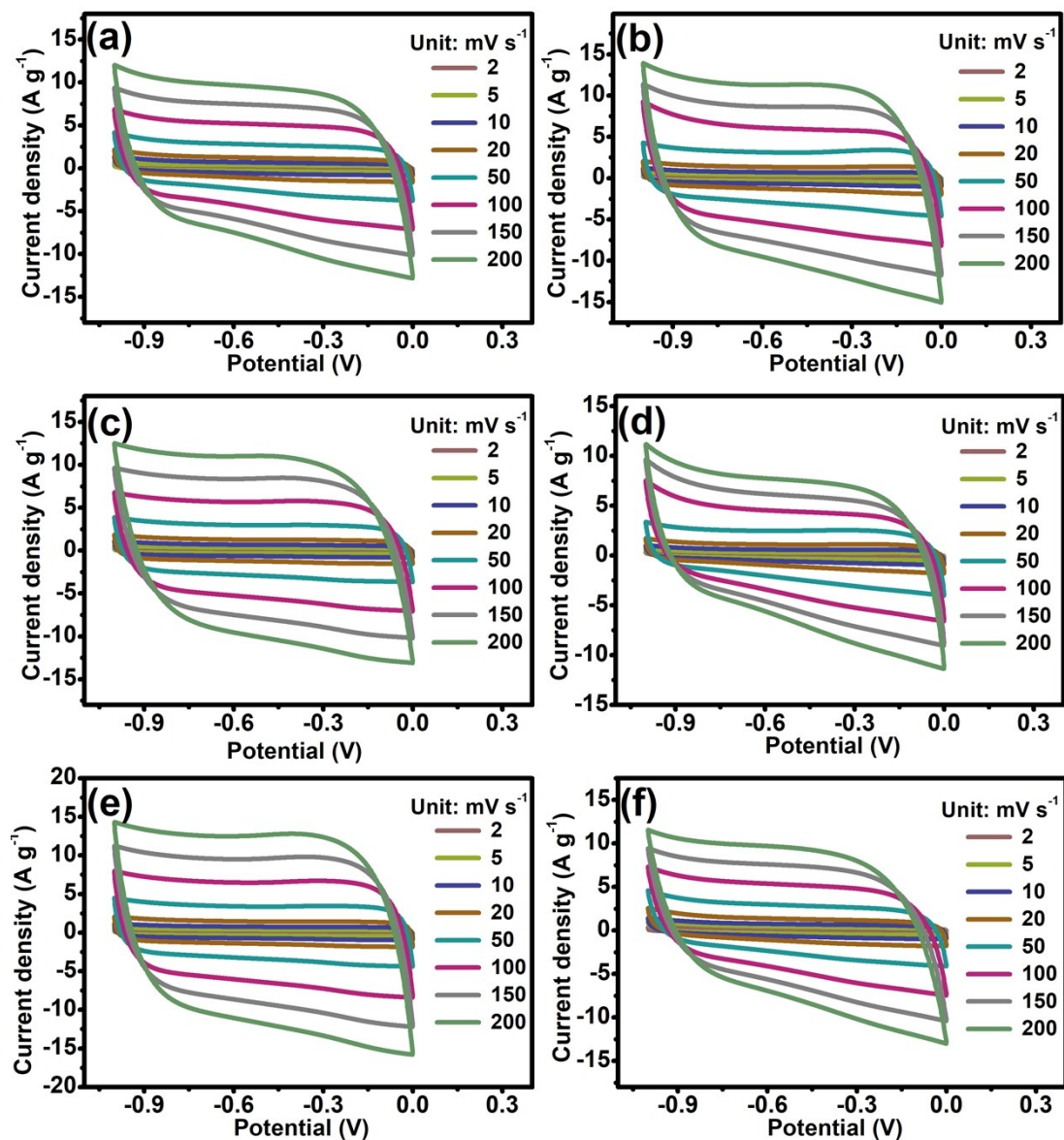


Fig. S4 (a) CV curves of all samples with the different sweep rates: (a) WDK-700-0, (b) WDK-700-0.5, (c) WDK-700-1.5, (d) WDK-700-2, (e) WDK-600-1, (f) WDK-800-1.

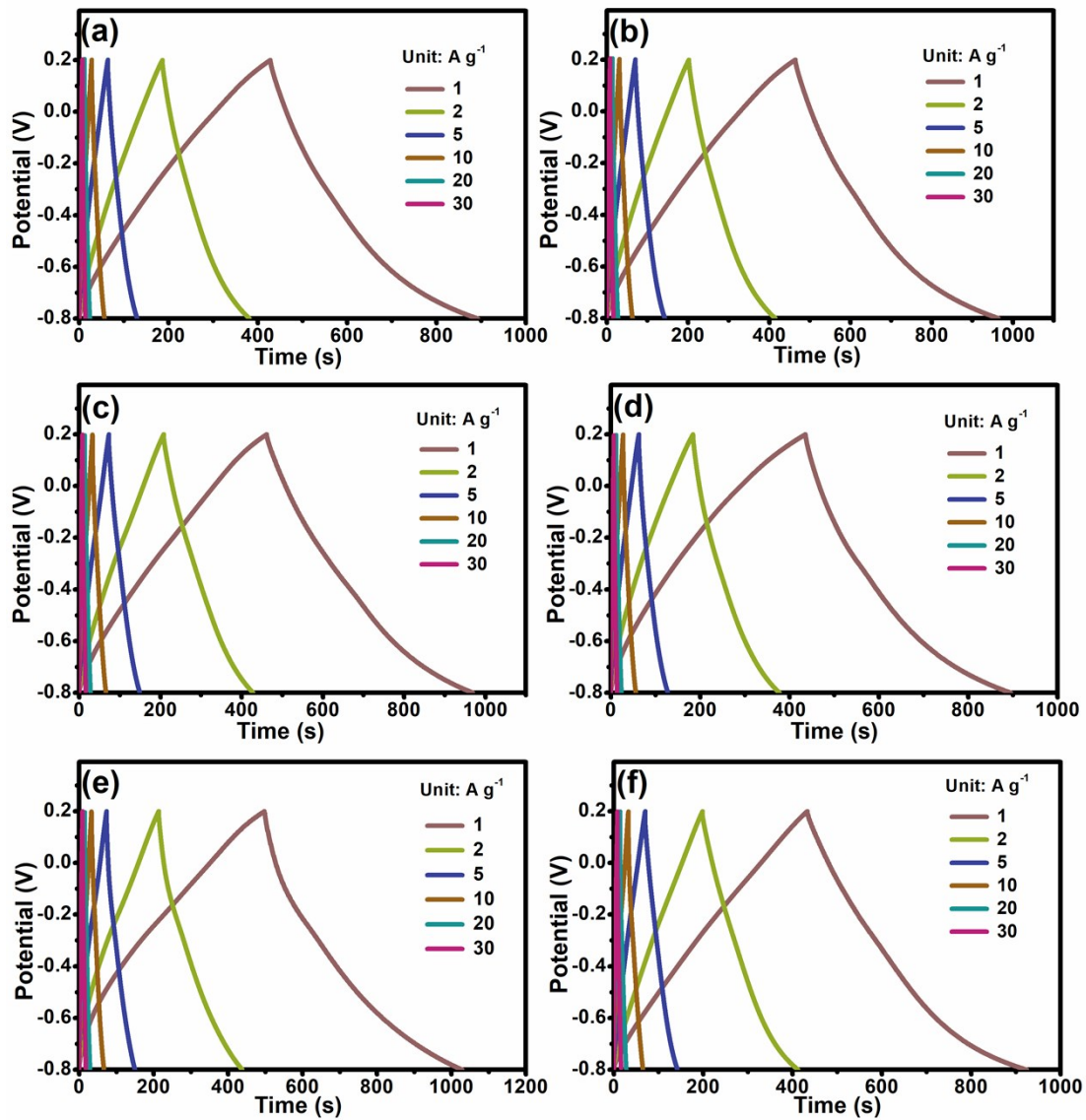


Fig. S5 GCD curves of all samples at various current densities from 1 to 30  $\text{A g}^{-1}$  in 1 mol  $\text{L}^{-1}$   $\text{H}_2\text{SO}_4$  electrolyte with the three-electrode system: (a) WDK-700-0, (b) WDK-700-0.5, (c) WDK-700-1.5, (d) WDK-700-2, (e) WDK-600-1, (f) WDK-800-1.

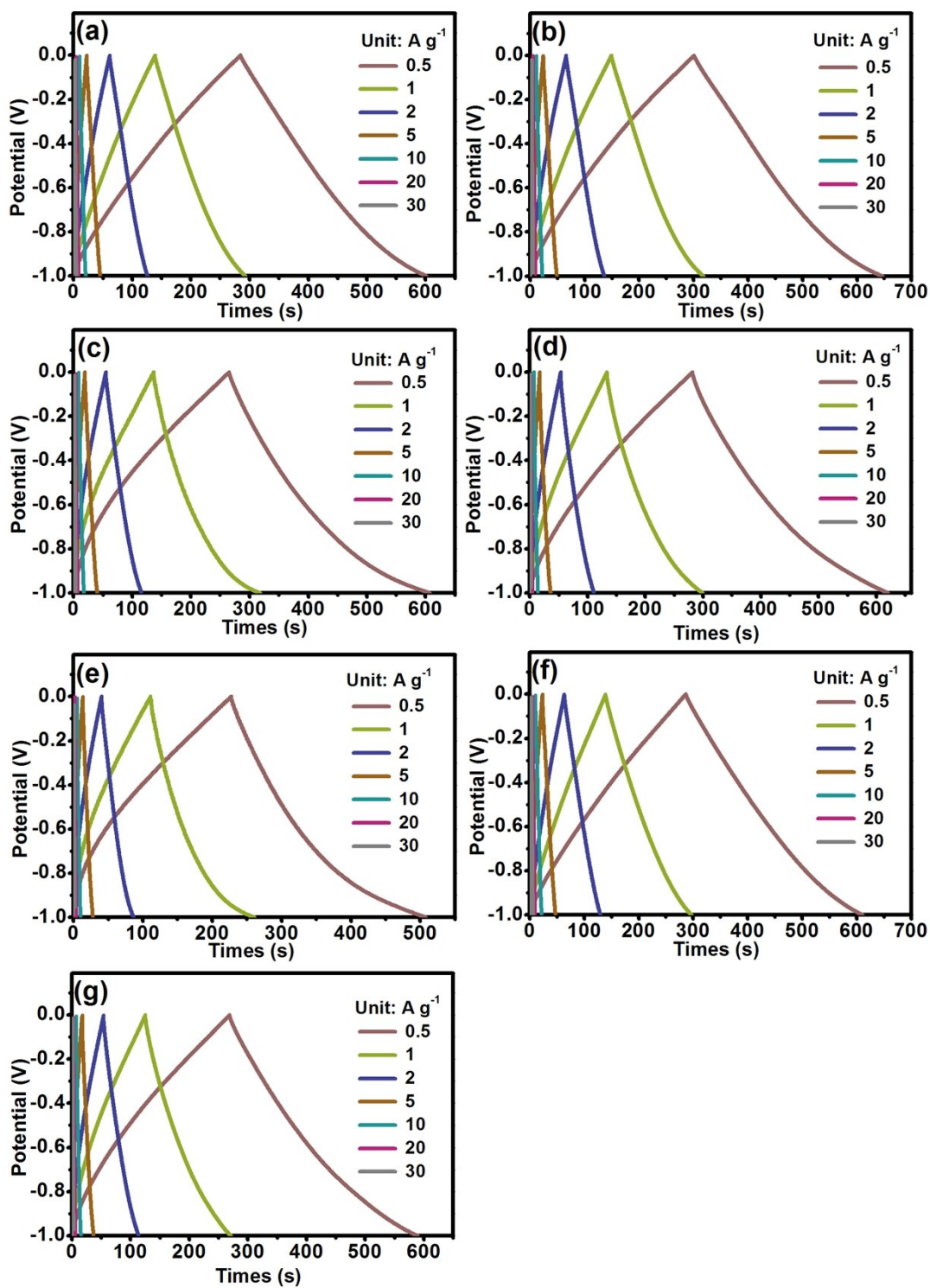
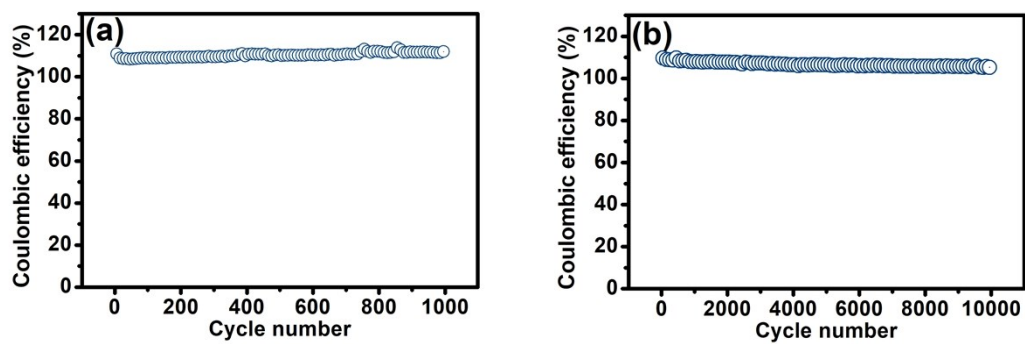


Fig. S6 GCD curves of all samples at various current densities from 1 to 30  $\text{A g}^{-1}$  in 1  $\text{mol L}^{-1}$   $\text{H}_2\text{SO}_4$  electrolyte with the two-electrode system: (a) WDK-700-0, (b) WDK-700-0.5, (c) WDK-700-1, (d) WDK-700-1.5, (e) WDK-700-2, (f) WDK-600-1, (g) WDK-800-1.

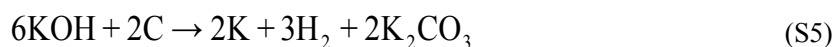


**Fig. S7** Coulombic efficiency of WDK-700-1 electrode at 1 A g<sup>-1</sup> for 1000 cycles (a) and Coulombic efficiency of WDK-700-1 electrode at 30 A g<sup>-1</sup> for 10000 cycles (b)



### The activator mechanism of KOH

Using KOH porogen is one effective way to create the micropores. It is generally believed that the productions in this progress below 700 °C are mainly H<sub>2</sub>, H<sub>2</sub>O, CO, CO<sub>2</sub>, K<sub>2</sub>O, and K<sub>2</sub>CO<sub>3</sub>.<sup>1</sup> This process consists of several simultaneous/continuous reactions as indicated in the following Equations (S1)-(S4). Moreover, at the activation temperature around 400 °C, owing to the dehydration of KOH, K<sub>2</sub>O has been produced (Equation (S1)).<sup>2</sup> Then H<sub>2</sub> and CO<sub>2</sub> could be generated as shown in the Equation (S2) and (S3). Hereafter, the K<sub>2</sub>O and CO<sub>2</sub> can be converted into K<sub>2</sub>CO<sub>3</sub> (Equation (S4)). And the reactions at 570 °C occur by following redox reaction (Equation (S5)):<sup>3</sup>



Next, the obtained K<sub>2</sub>CO<sub>3</sub> (Equation (4) and (5)) would be transformed into CO<sub>2</sub> and K<sub>2</sub>O (Equation (6)) at over than 700 °C, and K<sub>2</sub>O could be further reacted with the carbon to produce the metallic K (Equation (7)).<sup>4, 5</sup> Metallic K (Equation (5) and (7)) would intercalate into the carbon structure and expand the lattice leading to the increasing of pore volume. And the escape of H<sub>2</sub>, CO<sub>2</sub>, CO and H<sub>2</sub>O gas from carbon materials as the physical porogens change some micropores into mesopores thus enhancing the porosity.<sup>6</sup> After removing the inserted metallic K and K-containing compounds by the process of hydrochloric acid washing, the expanded carbon lattices cannot be recovered, thus reasonably developing the porosity of the materials.<sup>4, 7</sup>

**Table S1** Detailed quantitative element analysis data.

Sample	C <sub>1s</sub>	O <sub>1s</sub>	O <sub>1s</sub>				N <sub>1s</sub>	N <sub>1s</sub>			
			C=O	C-OH	C-O-C	COOH		N-6	N-5	N-Q	N-O <sub>x</sub>
WDK-700-0	80.9	17.34	0.29	0.31	0.29	0.11	1.76	0.28	0.28	0.19	0.26
WDK-700-0.5	78.35	20.09	0.33	0.25	0.24	0.17	1.56	0.31	0.47	0.16	0.06
WDK-700-1	85.3	12.93	0.18	0.34	0.29	0.19	1.77	0.14	0.40	0.32	0.14
WDK-700-1.5	85.95	12.62	0.17	0.29	0.34	0.20	1.43	0.23	0.33	0.27	0.17
WDK-700-2	82.93	15.68	0.20	0.32	0.31	0.17	1.40	0.22	0.32	0.28	0.18
WDK-600-1	79.41	19.1	0.25	0.33	0.31	0.12	1.49	0.28	0.31	0.28	0.13
WDK-800-1	89.9	7.89	0.16	0.30	0.32	0.21	2.21	0.16	0.40	0.28	0.16

**Table S2.** Comparison of electrochemical performances of the carbon materials synthesized from biomass in supercapacitors.

Materials	Surface area [m <sup>2</sup> g <sup>-1</sup> ]	Electrolyte	Capacitance [F g <sup>-1</sup> ]	E [Wh kg <sup>-1</sup> ]	P [kW kg <sup>-1</sup> ]	Reference
Walnut peel	2495.4	H <sub>2</sub> SO <sub>4</sub>	557.9 <sup>a; b</sup>	12.4	5.7	This study
Cellulose	859	H <sub>2</sub> SO <sub>4</sub>	328 <sup>a; c</sup>	–	–	[9]
Cotton	2436	KOH	283 <sup>a; b</sup>	–	–	[10]
Coconut Shell	2440	H <sub>2</sub> SO <sub>4</sub>	221.4 <sup>a; g</sup>	7.6	4.5	[11]
Chitosan	1582	KOH	252 <sup>a; c</sup>	–	–	[12]
Bagasse	2064	H <sub>2</sub> SO <sub>4</sub>	142 <sup>a; c</sup>	19.7	0.5	[13]
Human Hair	1306	KOH	340 <sup>a; b</sup>	45.3	2.2	[14]
Rice Husk	1768	KOH	233 <sup>a; f</sup>	8.36	–	[15]
Pomelo Peel	2725	KOH	342 <sup>a; e</sup>	9.4	0.1	[16]
Waste Air-laid Paper	1470	KOH	296 <sup>a; c</sup>	34.3	0.3	[17]
RF Resins	2178	KOH	222 <sup>d; c</sup>	10.1	8.0	[18]
Pomelo Peel	2191	KOH	342 <sup>a; b</sup>	17.1	3.8	[19]
Fungus	1103	KOH	360 <sup>a; b</sup>	22.0	–	[20]
NCAs	1626	KOH	354 <sup>a; e</sup>	–	–	[21]
Duckweeds	1636	KOH	315 <sup>a; b</sup>	8.3	0.1	[22]

<sup>(a)</sup>Capacitance with three-electrode system, <sup>(b)</sup> the current density of 1 A g<sup>-1</sup>, <sup>(c)</sup> the current density of 0.5 A g<sup>-1</sup>,  
<sup>(d)</sup> Capacitance with two-electrode system, <sup>(e)</sup> the current density of 0.2 A g<sup>-1</sup>, <sup>(f)</sup> the current density of 2 A g<sup>-1</sup>,  
<sup>(g)</sup> the current density of 5 A g<sup>-1</sup>.

## Notes and references

- 1 T. Otowa, R. Tanibata, and M. Itoh, *Gas separation & purification*, 1993, **7**, 241-245.
- 2 L. Qie, W. Chen, H. Xu, X. Xiong, Y. Jiang, F. Zou, X. Hu, Y. Xin, Z. Zhang and Y. Huang, *Energy Environ. Sci.*, 2013, **6**, 2497-2504.
- 3 M. Sevilla, A. B. Fuertes and R. Mokaya, *Energy Environ. Sci.*, 2011, **4**, 1400-1410.
- 4 J. Gañan, C. M. González-García, J. F. González, E. Sabio, A. Macías-García and M. A. Díaz-Díez, *Appl. Surf. Sci.*, 2004, **238**, 347-354.
- 5 Y. Sudaryanto, S. B. Hartono, W. Irawaty, H. Hindarso and S. Ismadji, *Bioresource Technol*, 2006, **97**, 734-739.
- 6 X. Wei, H. Zou and S. Gao, *Carbon*, 2017, **123**, 471-480.
- 7 X. Wei, Y. Li and S. Gao, *J. Mater. Chem. A*, 2017, **5**, 181-188.
- 8 H. Zhuo, Y. Hu, X. Tong, L. Zhong, X. Peng and R. Sun, *Ind. Crops Prod.*, 2016, **87**, 229-235.
- 9 P. Cheng, T. Li, H. Yu, L. Zhi, Z. Liu and Z. Lei, *J. Phys. Chem. C*, 2016, **120**, 2079-2086.
- 10 A. Jain, C. Xu, S. Jayaraman, R. Balasubramanian, J. Y. Lee and M. P. Srinivasan, *Microporous Mesoporous Mater.*, 2015, **218**, 55-61.
- 11 X. Deng, B. Zhao, L. Zhu and Z. Shao, *Carbon*, 2015, **93**, 48-58.
- 12 P. Hao, Z. Zhao, J. Tian, H. Li, Y. Sang, G. Yu, H. Cai, H. Liu, C. P. Wong and A. Umar, *Nanoscale*, 2014, **6**, 12120-12129.
- 13 W. Qian, F. Sun, Y. Xu, L. Qiu, C. Liu, S. Wang and F. Yan, *Energy Environ. Sci.*, 2014, **7**, 379-386.
- 14 X. He, P. Ling, M. Yu, X. Wang, X. Zhang and M. Zheng, *Electrochim. Acta*, 2013, **105**, 635-641.
- 15 Q. Liang, L. Ye, Z. H. Huang, Q. Xu, Y. Bai, F. Kang and Q. H. Yang, *Nanoscale*, 2014, **6**, 13831-13837.
- 16 J. Pu, C. Li, L. Tang, T. Li, L. Ling, K. Zhang, Y. Xu, Q. Li and Y. Yao, *Carbon*, 2015, **94**, 650-660.
- 17 H. Xuan, Y. Wang, G. Lin, F. Wang, L. Zhou, X. Dong and Z. Chen, *RSC Adv.*, 2016, **6**, 15313-15319.
- 18 C. Peng, J. Lang, S. Xu and X. Wang, *RSC Adv.*, 2014, **4**, 54662-54667.
- 19 C. Long, X. Chen, L. Jiang, L. Zhi and Z. Fan, *Nano Energy*, 2015, **12**, 141-151.
- 20 J. Zhang, G. Chen, Q. Zhang, F. Kang and B. You, *ACS Appl. Mat. Interfaces*, 2015, **7**, 12760-12766.
- 21 T. Wang, J. Zhang, Q. Hou, and S. Wang, *J. Alloys Compd.*, 2019, **771**, 1009-1017.